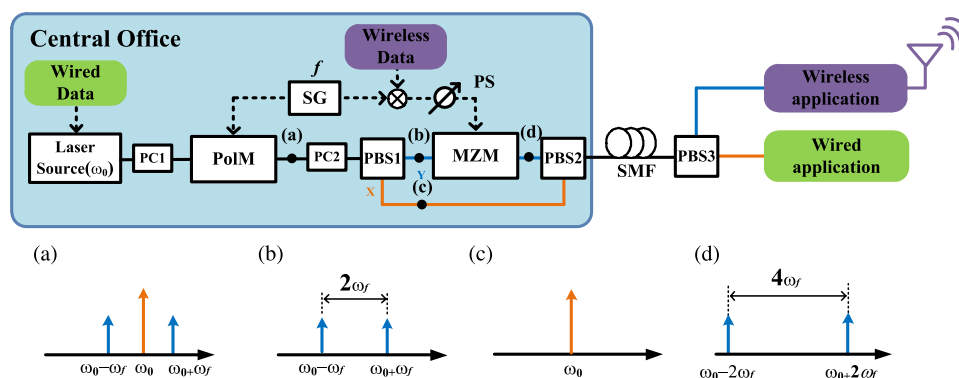


Hybrid OFDM and Radio-Over-Fiber Transport System Based on a Polarization Modulator

Volume 7, Number 5, October 2015

Ching-Hung Chang
Peng-Chun Peng
Han-Wen Gu
Chin-Wang Huang
Meng-Hsin Fang
Hsuan-Lun Hu
Po-Tso Shen
Chung-Yi Li
Hai-Han Lu



DOI: 10.1109/JPHOT.2015.2476839
1943-0655 © 2015 IEEE

Hybrid OFDM and Radio-Over-Fiber Transport System Based on a Polarization Modulator

Ching-Hung Chang,¹ Peng-Chun Peng,² Han-Wen Gu,² Chin-Wang Huang,²
Meng-Hsin Fang,² Hsuan-Lun Hu,² Po-Tso Shen,²
Chung-Yi Li,² and Hai-Han Lu²

¹Department of Electrical Engineering, National Chiayi University, Chiayi 600, Taiwan

²Department of Electro-Optical Engineering, National Taipei University of Technology,
Taipei 106, Taiwan

DOI: 10.1109/JPHOT.2015.2476839

1943-0655 © 2015 IEEE. Translations and content mining are permitted for academic research only.

Personal use is also permitted, but republication/redistribution requires IEEE permission.

See http://www.ieee.org/publications_standards/publications/rights/index.html for more information.

Manuscript received August 12, 2015; revised August 30, 2015; accepted September 1, 2015. Date of publication September 4, 2015; date of current version September 17, 2015. This work was supported in part by the Ministry of Science and Technology, Taiwan, under Contract NSC 101-2221-E-027-041-MY3, Contract MOST 104-2221-E-415-023, and Contract MOST 104-2221-E-027-072-MY3 and in part by the National Taipei University of Technology. Corresponding author: P.-C. Peng (e-mail: pcpeng@ntut.edu.tw).

Abstract: A hybrid orthogonal frequency-division multiplexing (OFDM) and quadruple-frequency radio-over-fiber (RoF) transport system is developed based on colorless optical polarization beam splitters and an optical polarization-arrangement technique. No optical filter is required to eliminate any specific optical wavelength from the hybrid transport system; the employed optical wavelength and central carrier frequency of the transmitted radio-frequency signal can be dynamically adjusted without alerting the transmission performance of the proposed hybrid transport system. To prove the concept of the quadruple-frequency technique, a 40-GHz millimeter-wave (MMW) signal quadrupled from a 10-GHz signal is experimentally demonstrated in an optical domain. Its advancement is then employed to experimentally accomplish a hybrid OFDM and quadruple-frequency RoF signal transmission over a 25-km span of single-mode fiber. The advancement of the hybrid transport system is evaluated and demonstrated by error-free transmissions and clear eye and constellation diagrams. This proposed system is a great candidate for greatly reducing the cost of simultaneously transmitting OFDM and MMW signals over optical access networks and makes it more practical to be employed.

Index Terms: Optical fiber communication, radio-over-fiber (RoF) system.

1. Introduction

Millimeter-wave (MMW) signals have been extensively utilized in various applications, such as broadband wireless communication, Atacama large millimeter arrays, MMW imaging, and terahertz applications. Given its great potential to deliver gigabit data streams, employing MMW signal transmissions to achieve next generation wireless networks is widely developed in the field of communication and radio-over-fiber (RoF) transport systems are particularly utilized to distribute MMW signals between a central office (CO) and base stations (BS) [1]–[3]. Furthermore, to realize low cost and high transmission performance in RoF-based optical wireless access networks, employing optical frequency up-conversion techniques to increase the central frequency of a radio-frequency (RF) signal to MMW range has also attracted much attention in optical

research [4]–[7]. For example, in [7], a photonic MMW-ultra-wideband signal generation technique is realized via directly frequency up-conversion using a dual-parallel MZM. Furthermore, if an RF signal is externally modulated with an optical carrier via a Mach–Zehnder modulator (MZM) and the MZM is biased at the null point to generate an optical carrier suppression (OCS) phenomenon in the output, the central frequency of the modulated RF signal can be up-converted two times after a detection of a photo detector (PD) [8]. Similarly, such OCS phenomena can be generated when a phase modulator (PM) is driving at a large modulation index [9]. Such two types of RoF transport systems will greatly improve the application of next generation wireless networks. Nevertheless, to achieve a proper carrier suppression index in PM- and MZM-based schemes, an electric amplifier with high-output power must be employed to boost the RF power level into a specific value before being modulated with the optical carrier; hence, a precise operation is required. Moreover, the frequency of the transmitted RF signal can only be doubled. To provide a quadruple-frequency up-conversion function in an RoF transport system, the MZM must be biased at a top operation point to suppress odd-order harmonic sidebands and must add an optical filter or an optical wavelength separator, such as an optical interleaver or an array waveguide grating (AWG), to eliminate the central carrier of the MZM output lightwave before feeding the remained lightwave into a PD [10]. Similarly, the PM-based quadruple-frequency technique also requires an optical filter or a wavelength separator to eliminate unwanted optical sidebands. These methods are inefficient and inflexible, because the passband window of an optical filter or an optical wavelength separator is fixed, and employing such devices to eliminate specific optical wavelength is inflexible; system performance cannot be ensured once the wavelength misalignment occurs. In parallel with the discussed schemes, employing direct-beating of two independent lasers to generate MMW signals are also developed [11], [12]. The central frequency of the generated MMW signal can be flexibly adjusted by modifying the wavelength spacing of the employed two lasers. Nevertheless, such schemes are difficult to be maintained and repaired because a slight change of the wavelength spacing between the employed lasers will significantly alter the central frequency of the generated MMW signal.

To simplify the operation of the optical wavelength alignment process in optical quadruple-frequency techniques and to provide a proper carrier suppression index, a quadruple-frequency technique is developed based on the optical polarization-arrangement technique, colorless passive devices, and the cooperation of a polarization modulator (PoIM) and a MZM. This technique is consequently employed to compose a hybrid orthogonal frequency-division multiplexing (OFDM) and a quadruple-frequency RoF transport system without employing an optical filter. With the assistance of the developed optical quadruple-frequency technique, the optical power of the generated second-order sidebands is 20 dB higher than the powers of the central carrier and the first-order sidebands. A 10-GHz RF signal can be colorlessly up-converted to the 40-GHz range in the proposed scheme. To prove the concept of the quadruple-frequency technique, a 40-GHz MMW signal quadrupled from a 10-GHz signal is experimentally demonstrated in optical domain. The outcomes of the experiment are employed to develop the proposed hybrid OFDM and quadruple-frequency RoF transport system. The advancement of the proposed system is evaluated and proved by proper bit error rate performance, clear eye, and constellation diagrams.

2. Operation Principle

Fig. 1 schematically illustrates the operation principle of the proposed system. In the system, a wired data is directly modulated with a distributed feedback-laser diode (DFB-LD) and the generated optical lightwave emitted at frequency ω_0 is polarized by a polarization controller (PC1) prior to polarization-modulation with a RF signal ω_f via a PoIM. The PC1 is employed to adjust the polarization state of the optical carrier; once the polarization state of the optical carrier is set to an angle of 45° relative to one principal axis of the PoIM, the lightwave is equally projected onto the two orthogonal polarization directions of the PoIM. As a result, the polarization directions of the optical central carrier and the first-order sidebands will remain in orthogonal states at the output of the PoIM. With the assistance of another PC (PC2) to align the polarization directions of the

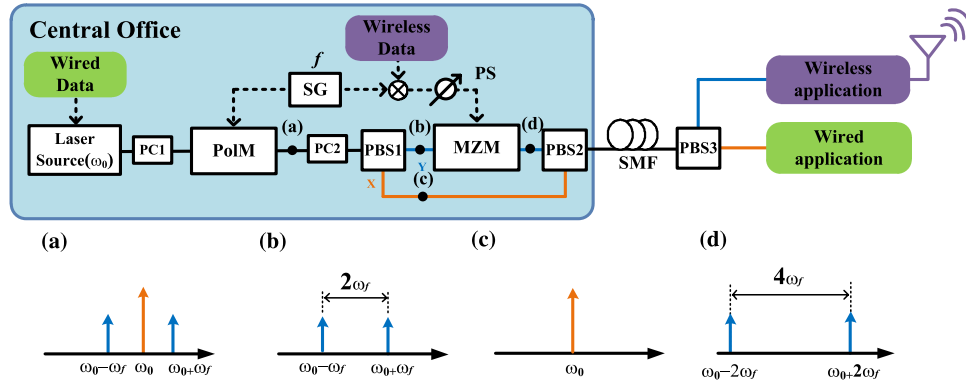


Fig. 1. Schematic diagram of the frequency-quadrupling technique based on polarization modulator (PoIM: polarization modulator, PC: polarization controller, SG: signal generator, PBS: polarization beam splitter, MZM: Mach-Zehnder modulator, PS: phase shifter, SMF: single-mode fiber).

optical carrier and the first-order sideband with the two principal axes of a polarization beam splitter (PBS), the optical carrier and the first-order sidebands can be separated and routed into two different output ports of the PBS [13]. The schematic spectrum diagrams of the downstream lightwave at the PBS input port and two output ports are shown in the Fig. 1(a)–(c), respectively. To obtain an optical quadruple-frequency phenomenon, the first-order sidebands located at $\omega_0 - \omega_f$ and $\omega_0 + \omega_f$ are fed into a MZM driven by an identical downstream RF signal, ω_f . By properly adjusting the bias point of the MZM to a null operation point, both input sidebands will generate a double sideband with suppressed carrier format at the MZM output. When an MZM is biased at a null operation point, the electric field of its output signal can be approximately expressed by [14]

$$E_{\text{out}}(t) \approx J_1(\beta)E_0\{\cos[(\omega_0 - \omega_f)t - \varphi] + \cos[(\omega_0 + \omega_f)t + \varphi]\} \quad (1)$$

where E_0 is the electric field amplitude, β is the modulation index, and φ is the phase of the electrical signal. When the first-order sidebands of the PoIM output are fed into the MZM, each will generate two new sidebands located at $\omega_0 - 2\omega_f$ and ω_0 as well as ω_0 and $\omega_0 + 2\omega_f$, respectively. The electric field of the MZM output signal can be approximately expressed by

$$E_{\text{MZM.out}}(t) \approx J_1(\beta_1)J_1(\beta_2)E_0 \cos\left[(\omega_0 - 2\omega_f)t - \varphi_1 - \varphi_2 - \frac{\pi}{2}\right] + J_1(\beta_1)J_1(\beta_2)E_0 \cos\left[(\omega_0 + 2\omega_f)t + \varphi_1 + \varphi_2 - \frac{\pi}{2}\right] \quad (2)$$

where β_1 and β_2 are the modulation index of the PoIM and MZM, respectively, and φ_1 and φ_2 are the phase of the electrical signal fed into the PoIM and MZM, respectively. Once the initial phase of the RF signal is $\pi/2$ shifted by a phase shifter (PS) prior to insertion into the MZM, the MZM output sidebands located at ω_0 will eliminate each other because both have the same intensity but are pi radians out of phase. The remaining two sidebands located at $\omega_0 - 2\omega_f$ and $\omega_0 + 2\omega_f$, as shown in Fig. 1(d), will be able to achieve a four times frequency up-conversion process at the receiver PD.

To communicate both wired and wireless MMW signals to their destinations, the central carrier of the PoIM output is routed from PBS1 to PBS2, and MZM output is fed into another port of the PBS2 prior to transmission via a single mode fiber (SMF). After communicating over a span of SMF, the transmitted central carrier and two sidebands can be separated again by a PBS (PBS3) at the end of the SMF because they have different polarization states. The central carrier embedded wired data can be employed for wired application, and the two sideband-embedded MMW wireless data can be employed for wireless application. In the proposed approach, the baseband and quadruple-frequency microwave signals are generated by cascading a PoIM with a MZM; no optical filter is required to separate the downstream lightwaves and no wavelength misalignment issue needs to be concerned.

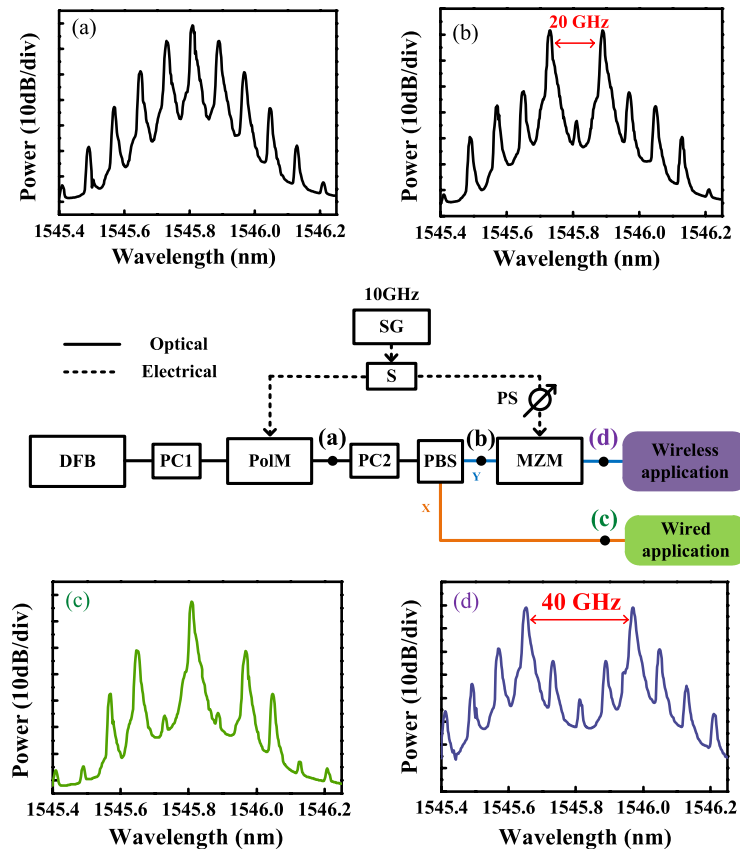


Fig. 2. Experimental setup of the proposed scheme for the case of a 10-GHz modulation frequency (S: splitter and DFB: distributed-feedback laser).

To prove the concept of the proposed system, a quadruple-frequency 40-GHz MMW signal generation is arranged based on the architecture shown in Fig. 2. Similar to the architecture shown in the Fig. 1, an optical carrier generated by a DFB-LD is adjusted by a PC and then polarization-modulated with a 10-GHz RF signal via a PoIM. The PoIM output lightwave is separated by a PBS before being remodulated with the same 10-GHz RF signal via a MZM. The optical spectra measured at the PBS input port and two output ports are shown in Fig. 2(a)–(c), respectively. These three figures show that the first-order sidebands of the PoIM output are separated and routed to the PBS-y-axis output port before being fed into the MZM, and the central carrier and other sidebands are directed into the PBS-x-axis output port for wired application. When the MZM is biased at the null operation point to suppress odd-order sidebands and the phase of the 10-GHz RF signal is shifted by $\pi/2$, the two new sidebands generated at the central area are automatically eliminated by each other. A DSB output formant is generated, as shown in Fig. 2(d). The frequency spacing between these two sidebands is 40 GHz (4×10 GHz). Taking advantage of this property in MMW over fiber transport systems can dramatically lower the bandwidth requirements of the optical modulator and electrical drives and can greatly reduce the cost of the system and make it more practical for use.

3. Experimental Setup and Results

Fig. 3 shows the experimental setup of the proposed hybrid OFDM and quadruple-frequency RoF transport system. In the CO, a DFB-LD with a central wavelength of 1545.8 nm was directly modulated by an OFDM data stream with a data rate of 1.25 Gbps, 16 subcarriers, and quadrature phase-shift keying (QPSK) modulation format. The OFDM scheme is a promising

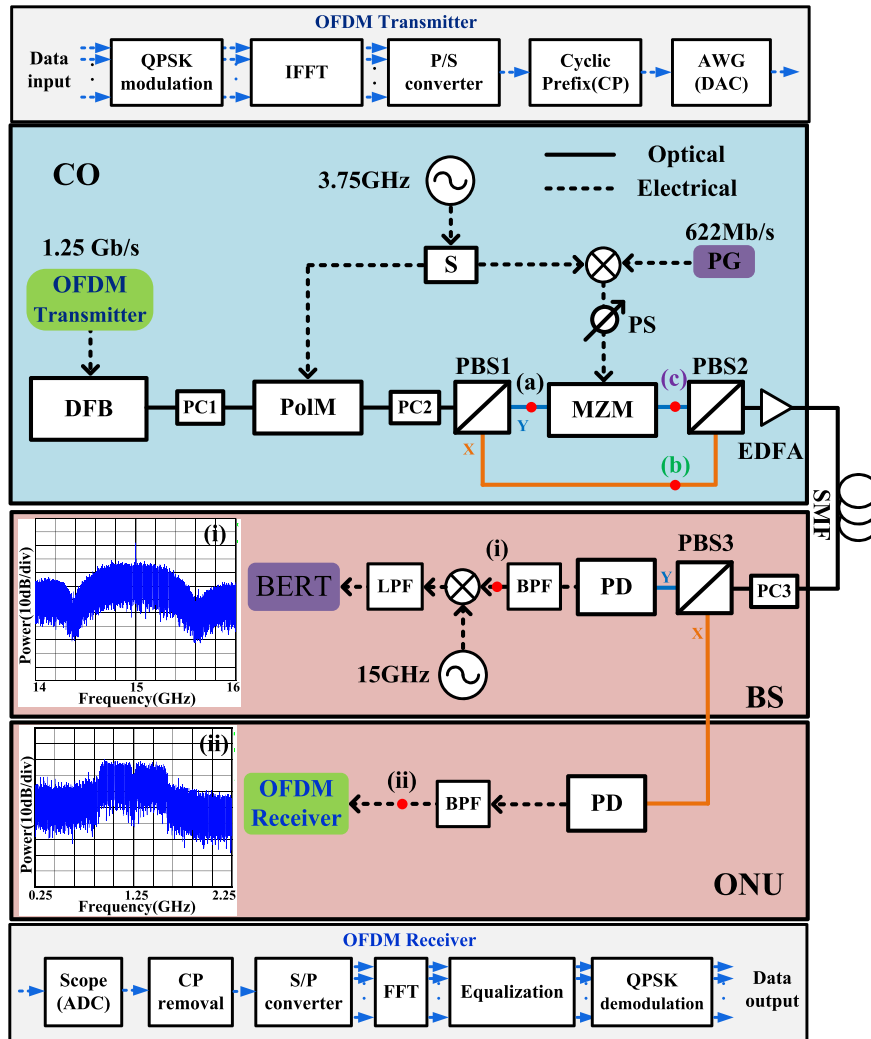


Fig. 3. Schematic diagram of the proposed hybrid transport system (CO: central office, OFDM: orthogonal frequency-division multiplexing, QPSK: quadrature phase-shift-keying, IFFT: inverse fast Fourier transform, AWG: arbitrary waveform generator, EDFA: erbium-doped fiber amplifier, PD: photodetector, BPF: band-pass filter, LPF: low-pass filter, BERT: bit error rate tester).

technology, owing to its extremely high spectrum efficiency and robust dispersion tolerance, for improving transmission performance and capabilities in transport systems [15], [16]. The top inset of the Fig. 3 shows the OFDM transmitter, which consists of serial-to-parallel conversion, QPSK modulation, inverse fast Fourier transform (IFFT), parallel-to-serial conversion, cyclic prefix (CP) insertion, and digital-to-analog conversion (DAC). IFFT size is set to 256 and the sampling rate and digital-to-analog converter resolution of the employed arbitrary waveform generator (AWG, Tektronix AWG7102) are 10 Gsample/s and 8 bits, respectively. After being driven by the OFDM signal, the DFB-LD output is then polarized by a PC (PC1) to have an angle of 45° relative to a principal axis of a PoIM prior to being fed into the PoIM. For the wireless data transmission, because of the absence of high-frequency MMW demodulation devices, the carrier frequency of the downstream RF signal is set to 3.75 GHz instead of 10 GHz. To achieve a quadruple-frequency function, the 3.75-GHz sinusoid carrier is split into two branches. One branch is amplified by an electrical amplifier (EA) and then applied to the PoIM.

Another branch of the RF carrier is mixed with a 622-Mbps on-off keying (OOK) data stream with a pseudo random bit sequence (PRBS) and word length of $2^{31} - 1$. The phase of the mixed

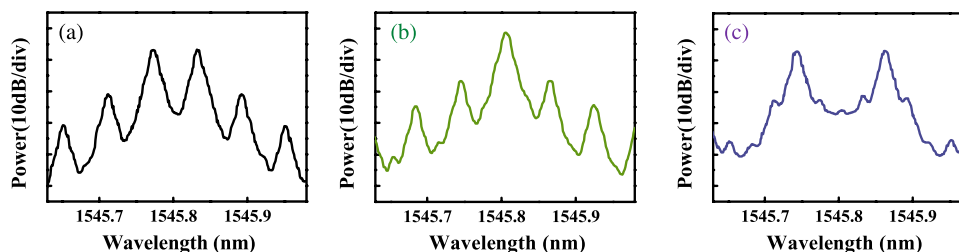


Fig. 4. Optical spectra measured at point (a)–(c) in Fig. 3.

RF signal is then adjusted by a PS and amplified by an EA before being applied to a MZM connected at the PBS1-y-axis output port. Meanwhile, the PBS1 input port is connected to the PoIM output via a PC (PC2) and the PBS1-x-axis output port is connected to the x-axis input port of the second PBS (PBS2). PC2 is used to align the polarization directions of the PoIM output lightwave with two principal axes of the PBS1, so that the odd-order sidebands of the PoIM output will be routed to the y-axis output port of the PBS1. The others are routed to the x-axis output port of the PBS1. The optical spectra measured at the PBS1-y-axis and x-axis output ports are shown in Fig. 4(a) and (b), respectively. The odd-order and even-order sidebands are separated apparently. In the experiment, the cost of each PBS is less than 200 dollar. Comparing with employing narrow-band optical filters to separate the transmitted optical signals, utilizing the colorless PBSs to achieve the same work is cost effective.

When the odd-order sidebands of the PoIM output are remodulated with the 622-Mbps/3.75-GHz RF signal at the MZM, the MZM is biased at the null operation point to suppress the even-order sidebands of the remodulated lightwaves. The MZM output is then fed into the y-axis output port of the PBS2 to recombine with the lightwave from the x-axis output port of the PBS1. As shown in Fig. 4(c), an optical DSB modulation format is measured at the MZM output port. The two sidebands located at the central carrier of the downstream lightwave are eliminated. More than 19 dB carrier suppression ratio between the remained sidebands and the central carrier is achieved. The frequency spacing of the remained two sidebands is exactly four times the downstream RF signal. When the OFDM signal and quadruple-frequency RoF signal are combined at the PBS2, they are amplified by an erbium-doped fiber amplifier (EDFA) before being communicated over a 25-km span of SMF to a BS, where the polarization states of the downstream lightwave is adjusted with respect to two principal axes of a PBS (PBS3) by a PC (PC3), and separated again by the PBS3. The wireless data routed to the y-axis output port of the PBS3 is directly detected by a 20-GHz PD and filtered by a band-pass filter (BPF). The electrical spectrum measured at the PD output port is presented in Fig. 3(i). The desired four times frequency up-conversion process is achieved and the appearance of a clear signal at the 15-GHz range is evidence. Although the polarization angles of propagating signals in a random birefringence of buried optical fibers may typically cause $2 \sim 10^\circ$ fluctuation, a dynamic polarization control can be utilized to compensate the polarization fluctuations [17]. To evaluate the transmission performance of the wireless data, the obtained 622-Mbps/15-GHz RF signal is down-converted to the baseband by mixing with a 15-GHz sinusoidal signal and is analyzed by a bit error rate tester (BERT) after being filtered by a low-pass filter (LPF). The measured bit error rate (BER) curves and relative eye diagrams of the quadruple-frequency RoF signal in back-to-back (BTB) and 25-km SMF transmission scenarios are shown in Fig. 5. Error free transmissions are achieved simultaneously at both scenarios, and the power penalty between each is below 1 dB. The proper BER performance and clear and open eye diagrams are great evidence that prove the ability of the proposed system to provide great quality for quadruple-frequency RoF signal transmissions.

Aside from the RoF signal transmission, a PD connected to the x-axis output port of the PBS3 detects the OFDM signal embedded at the central carrier of the downstream lightwave. The obtained OFDM signal is then fed into an OFDM receiver after being filtered by a BPF. Inside the OFDM receiver, the waveform of the received signal is captured by a real-time scope

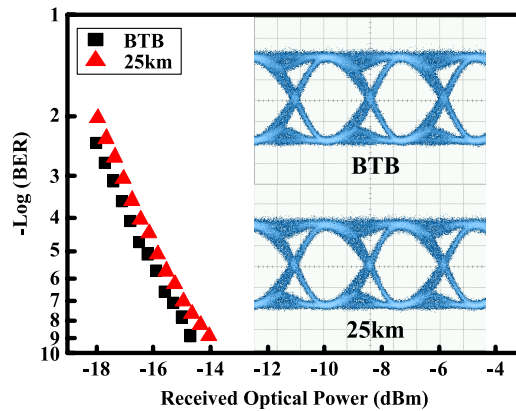


Fig. 5. Measured BER curves and eye diagrams of quadruple-frequency signals.

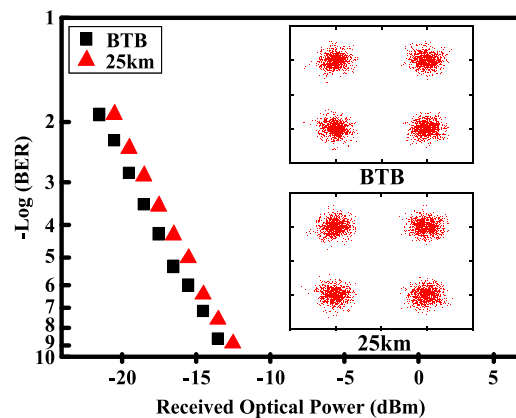


Fig. 6. Measured BER curves and constellation diagrams for 1.25-Gbps QPSK-OFDM signals.

(Tektronix CSA 7404B) with a 20-GS/s sampling rate and a 3-dB bandwidth of 4 GHz. Consequently, the OFDM signal is demodulated using an offline Matlab digital signal processing program. Due to the perfectly orthogonal polarization states between the central carrier and the second-order sidebands of the downstream lightwave, even the downstream lightwave is remodulated with RF signal via a PoIM and split, recombined, and re-split by PBS1, PBS2, and PBS3; the OFDM signal embedded at the optical central carrier still can be properly withdrawn by the PBS3 and clearly measured at the receiver end, as illustrated in Fig. 3(ii). The obtained BER curves and QPSK constellation diagrams in BTB and 25-km transmission scenarios are shown in Fig. 6. Error-free transmissions and clear constellation diagrams are obtained in both scenarios. Only a small power penalty of 0.3 dB presents between both transmission results. The experimental results of both OFDM and RoF signal transmissions demonstrate the ability of the proposed system to utilize a signal optical carrier to simultaneously and colorlessly accomplish optical OFDM and quadruple-frequency RoF signal transmissions without employing any optical filter to assist the signal detections. Even the wavelength of the optical carrier or the central frequency of the transmitted RF signal is modified; the proposed hybrid transport system is still able to properly accomplish its function.

4. Conclusion

A hybrid OFDM and quadruple-frequency RoF transport system is developed based on a colorless frequency quadrupling technique and optical polarization-arrangement technique. With the cooperation of a PoIM, a MZM, and PBSs, the frequency of a transmitted RF signal can be

colorlessly up-converted four times in the optical domain. An optical suppression ration higher than 20 dB is achieved experimentally for a 40-GHz MMW over-fiber signal without employing an optical filter. Taking advantage of the quadruple-frequency technique in the proposed hybrid OFDM and quadruple-frequency RoF transport system, both OFDM and RoF signals are successfully embedded in an optical carrier before being simultaneously transmitted over a 25-km span of SMF to a BS. The downstream lightwave including a central carrier and two main sidebands is separated by a colorless PBS prior to detection by an OFDM receiver and RoF receiver. The transmission performance of the OFDM signal embedded at the central carrier of the downstream lightwave is proven by great BER performances and clear constellation diagrams. The frequency of the RoF signal embedded at the two main sidebands of the downstream lightwave is successfully up-converted four times at the RoF receiver without employing an optical filter. The transmission performance of the quadruple-frequency RoF signal is also proven by great BER values and open eye diagrams. These results are great evidence to prove the ability of the proposed system to colorlessly provide great quality hybrid OFDM and quadruple-frequency RoF signal transmissions.

References

- [1] J. J. Vegas Olmos, T. Kuri, and K. I. Kitayama, "Reconfigurable radio-over-fiber networks: Multiple-access functionality directly over the optical layer," *IEEE Trans. Microw. Theory Tech.*, vol. 58, no. 11, pp. 3001–3010, Nov. 2010.
- [2] Y. T. Hsueh, M. F. Huang, S. H. Fan, and G. K. Chang, "A novel lightwave centralized bidirectional hybrid access network: Seamless integration of RoF with WDM-OFDM-PON," *IEEE Photon. Technol. Lett.*, vol. 23, no. 15, pp. 1085–1087, Aug. 2011.
- [3] C. Lim *et al.*, "Fiber-wireless networks and subsystem technologies," *J. Lightw. Technol.*, vol. 28, no. 4, pp. 390–405, Feb. 2010.
- [4] C. W. Chow, C. H. Yeh, J. Y. Sung, and C. W. Hsu, "Wired and wireless convergent extended-reach optical access network using direct-detection of all-optical OFDM super-channel signal," *Opt. Exp.*, vol. 22, no. 25, pp. 30 719–30 724, Dec. 2014.
- [5] H. T. Huang *et al.*, " 2×2 MIMO OFDM-RoF system employing LMS-based equalizer with I/Q imbalance compensation at 60 GHz," *IEEE Photon. J.*, vol. 6, no. 3, Jun. 2014, Art. ID. 7200307.
- [6] P. T. Shin *et al.*, "Optical millimeter-wave signal generation via frequency 12-tupling," *J. Lightw. Technol.*, vol. 28, no. 1, pp. 71–78, Jan. 2010.
- [7] W. Li, L. X. Wang, J. Y. Zheng, M. Li, and N. H. Zhu, "Photonic MMW-UWB signal generation via DPMZM-based frequency up-conversion," *IEEE Photon. Technol. Lett.*, vol. 25, no. 19, pp. 1875–1878, Oct. 2013.
- [8] C. T. Lin, J. Chen, S. P. Dai, P. C. Peng, and S. Chi, "Impact of nonlinear transfer function and imperfect splitting ratio of MZM on optical up-conversion employing double sideband with carrier suppression modulation," *J. Lightw. Technol.*, vol. 26, no. 15, pp. 2449–2459, Aug. 2008.
- [9] Y. T. Hsueh, H. C. Chien, A. Chowdhury, J. Yu, and G. K. Chang, "Performance assessment of radio links using millimeter-wave over fiber technology with carrier suppression through modulation index enhancement," *J. Opt. Commun. Netw.*, vol. 3, no. 3, pp. 254–258, Mar. 2011.
- [10] M. F. Huang, J. Yu, Z. Jia, and G. K. Chang, "Simultaneous generation of centralized lightwaves and double/single sideband optical millimeter-wave requiring only low-frequency local oscillator signals for radio-over-fiber systems," *J. Lightw. Technol.*, vol. 26, no. 15, pp. 2653–2662, Aug. 2008.
- [11] L. G. Yang *et al.*, "Coding for stable transmission of W-band radio-over-fiber system using direct-beating of two independent lasers," *Opt. Exp.*, vol. 22, no. 21, pp. 26 092–26 097, Oct. 2014.
- [12] C. W. Chow, J. Y. Sung, and C. H. Yeh, "A convergent wireline and wireless time-and-wavelength-division-multiplexed passive optical network," *IEEE Photon. J.*, vol. 7, no. 3, Jun. 2015, Art. ID. 7902107.
- [13] A. L. Campillo and F. Bucholtz, "Chromatic dispersion effects in analog polarization-modulated links," *Appl. Opt.*, vol. 45, no. 12, pp. 2742–2748, Apr. 2006.
- [14] J. Zhang, H. Chen, M. Chen, T. Wang, and S. Xie, "A photonic microwave frequency quadrupler using two cascaded intensity modulators with repetitious optical carrier suppression," *IEEE Photon. Technol. Lett.*, vol. 19, no. 14, pp. 1057–1059, Jul. 2007.
- [15] G. R. Lin, Y. C. Chi, and J. Chen, "Using a L-band weak-resonant-cavity FPLD for subcarrier amplitude pre-leveled 16-QAM-OFDM transmission at 20 Gbit/s," *J. Lightw. Technol.*, vol. 31, no. 7, pp. 1079–1087, Apr. 2013.
- [16] C. C. Wei, C. T. Lin, and C. Y. Wang, "PMD tolerant direct-detection polarization division multiplexed OFDM systems with MIMO processing," *Opt. Exp.*, vol. 20, no. 7, pp. 7316–7322, Mar. 2012.
- [17] L. Xu *et al.*, "A new orthogonal labeling scheme based on a 40-Gb/s DPSK payload and a 2.5-Gb/s PoSK label," *IEEE Photon. Technol. Lett.*, vol. 17, no. 12, pp. 2772–2774, Dec. 2005.